ChemComm

Blue Circularly Polarized Luminescent Amorphous Molecules with Single-handed Propeller Chirality Induced by Circularly Polarized Light Irradiation

Journal:	*ChemComm*
Manuscript ID	CC-COM-12-2020-007898.R1
Article Type:	Communication

COMMUNICATION

Blue Circularly Polarized Luminescent Amorphous Molecules with Single-handed Propeller Chirality Induced by Circularly Polarized Light Irradiation

Received 00th January 20xx,
Accepted 00th January 20xx

DOI: 10.1039/x0xx00000x

Zhaoming Zhang,[a] Takunori Harada,[b] Adriana Pietropaolo,[c] Yuting Wang,[a] Yue Wang,[a, †] Xiao Hu,[d] Xuehan He,[d] Hui Chen,[d] Zhiyi Song,[a] Masayoshi Bando[a] and Tamaki Nakano*[a,e]

Preferred-handed propeller conformation was induced by circularly polarized light irradiation to three amorphous molecules with trigonal symmetry, and the molecules with induced chirality efficiently exhibited blue circularly polarized luminescence. In both chirality induction and luminescence, chirality appeared to be amplified due to intermolecular interactions through π-stacking.

Optically active molecules and polymers are generally prepared using chiral compounds as chirality source where chirality information is transferred from the source to products through intermolecular interactions.[1-3] While polarized light (CPL) can also be used as chirality source for asymmetric synthesis,[4-8] the extent of asymmetry achieved by CPL irradiation is very low in most examples,[6-8] and only limited reports have presented high preferred-handedness of the products.[9-13] We herein present the introduction of efficient asymmetry to the three-armed, star-shaped, blue-luminescent molecules (S1, S2, and S3 in **Fig. 1**)[14] through chirality amplification by CPL irradiation, leading to preferred-handed propeller conformation.

CPL-irradiation-based helical chirality induction has been reported for polyfluorene derivatives in which chirality induction occurs through enantiomer-selective rotation of axially chiral biphenyl units comprising the main chain (**Scheme 1**).[15-19] Biphenyl has a twisted conformation in the ground state and is transformed to a coplanar conformation in excited states through rotation around the single bond, and if one of right- and left-handed twists is preferentially excited by CPL irradiation, the population of the un-excited twist increases, which leads to an optically active product (twist-sense-selective excitation).[20-23] In the present work, this principle was extended to axially chiral structures in S1, S2, and S3 including the *N*-phenylcarbazole moieties.

Also, it should be emphasized that efficient chirality induction generally requires highly-ordered intermolecular structures such as crystalline β-phase of polyfluorenes[15,16] and crystal surface of small molecules.[18] While CPL-based chirality induction to polymers bearing azobenzene moieties is also known where the mechanism may not be based on enantiomer-selective excitation of biphenyl units, liquid crystallinity plays an important role in chirality induction also in such cases.[24-30] In a sharp contrast, S1, S2, and S3 have been designed as amorphous, luminescent molecules having no intermolecular order as organic light emitting diode (OLED) candidates so that molecular ordering does not alter color and efficiency of their luminescence, and nevertheless, highly efficient chirality induction was attained where chirality was amplified through only local π-stacking interactions in the present work.

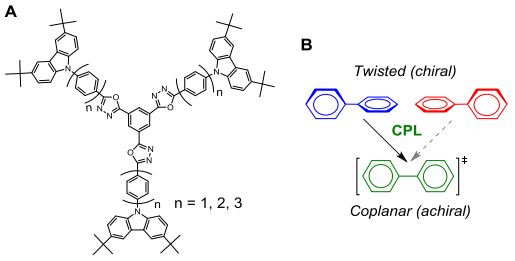

S1 n = 1; **S2** n = 2 ; **S3** n = 3

Fig. 1. Structures of star-shaped oligomers (**S1**, **S2**, and **S3**) [A] and enantiomer-selective photoexcitation inducing twisted-coplanar transition of biphenyl [B].

Axial chirality is possible for S1, S2, and S3 around the single bonds connecting 3,6-di-*t*-butyl-9H-carbazole-9-yl groups, benzene-1,4-diyl groups, 1,3,4-oxadiazole-2,5-diyl groups, and benzene-1,3,5-triyl group. Although conformational dynamics of the molecules in solution is extremely fast in solution, rotational freedom of the single bonds will be suppressed in the solid state. The chirality induction experiments were hence conducted in the solid state using thin film samples.

Thin films samples of S1, S2, and S3 were prepared by casting their chloroform solutions onto a quartz plate and were irradiated with CPL under nitrogen atmosphere. While all the as-cast films were

[a] *Institute for Catalysis (ICAT) and Graduate School of Chemical Sciences and Engineering, Hokkaido University, N21W10, Kita-ku, Sapporo 001-0021, Japan E-mail: tamaki.nakano@cat.hokudai.ac.jp.*
[b] *Department of Integrated Science and Technology, Faculty of Science and Technology, Oita University, Dannoharu, 700, Oita City 870-1192, Japan*
[c] *Dipartimento di Scienze della Salute, Università di Catanzaro, Viale Europa, 88100 Catanzaro, Italy*
[d] *School of Materials Science & Engineering, Nanyang Technological University, Singapore.*
[e] *Integrated Research Consortium on Chemical Sciences (IRCCS), ICAT, Hokkaido University, Sapporo 001-0021, Japan*
† *Present address: Lanzhou Institute of Chemical Physics, Chinese Academy of Sciences, Tianshui Middle Road, Lanzhou, Gansu 730000, P.R. China.*
Electronic Supplementary Information (ESI) available: [details of any supplementary information available should be included here]. See

circular dichroism (CD)-silent before irradiation, clear CD bands appeared on CPL irradiation to the films, and right- and left-handed CPL led to almost mirror image CD spectra (Fig. 2 A-1, B-1, C-1), indicating that CPL induced a chiral conformation to the molecules. CD intensity saturated within 300-400 min of irradiation (Fig. S2 in ESI). In addition, the sign of CD was reversibly switched by changing chirality of CPL (chirality switching) (Fig. S1 in ESI).

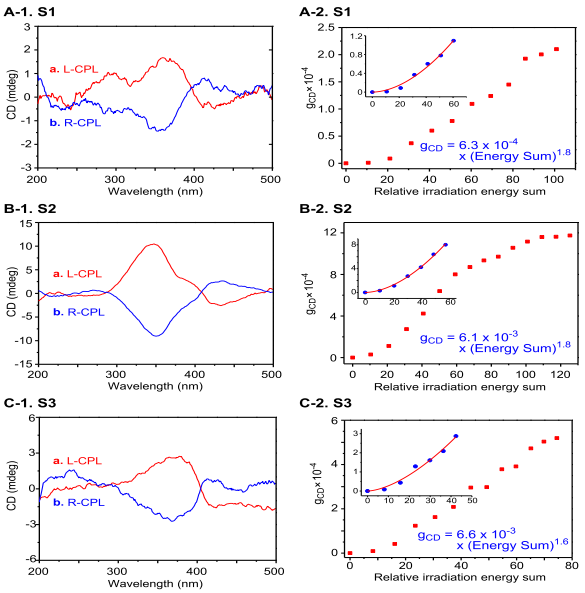

Fig. 2. CD spectra induced by L-CPL irradiation (a) and R-CPL irradiation (b) for S1 [A-1], S2 [B-1], and S3 [C-1] and g_{CD}-vs.-relative irradiation energy sum plots with curve fitting results (inset plots) for S1 [A-2], S2 [B-2], and S3 [C-2].

Also, absorbance spectra showed a gradual decrease in intensity (hypochromism) and change in shape along with the increase in CD intensity (Fig. S2 in ESI). The spectral changes are ascribed to a change in the average dihedral angle around single bonds which has been clarified for biphenyl molecule by combined theoretical and experimental studies.[32] The hypochromism may also be due to π-stacking of the molecules[33] which was facilitated through conformational transition facilitated by CPL irradiation. Such changes in absorbance have been observed for other systems of CPL-based chirality induction.[15-19] Indeed, the chemical structures of the molecules were not affected by irradiation as supported by IR spectral analyses (Fig. S3 in ESI).

CD intensity is discussed in terms of the Kuhn's anisotropy factor[34] for absorbance ($g_{CD} = 2(\varepsilon_L - \varepsilon_R)/(\varepsilon_R + \varepsilon_L)$ where ε_R and ε_L are molar absorptivities toward left-handed and right-handed CPL's, respectively) to eliminate the influence of absorbance intensity. Fig. 2 A-2, B-2, and C-2 show the plots of g_{CD} observed on L-CPL irradiation against relative irradiation energy sum (or relative absorbed dose) at 365 nm whose definition is found in ESI. The g_{CD}-vs.-energy sum plots do not show first-order type relations, but the early stages of chirality induction can be well approximated with power functions indicated within the figures. These findings strongly suggest that chirality is amplified during CPL irradiation. This aspect is further supported by the maximum g_{CD} values of the three molecules which were +2.2 x 10^{-4} at 368 nm (S1), +1.2 x 10^{-3} at 368 nm (S2), and +5.5 x 10^{-4} at 375 nm (S3) after saturation of CD intensity upon L-CPL irradiation. Aromatic compounds at 100% e.e. generally show g_{CD} values of 10^{-3} to 10^{-4} order,[7,19] and g_{CD} values attainable based only on chirality of CPL without amplification therefore are of 10^{-6} to 10^{-8} order. This is because the maximum e.e. values (γ_{PSS}) attainable at photo stationary state is known to follow the equation, γ_{PSS} = 1/2 $g_{CD(100\%\ e.e.)}$ x 100 %, which leads to maximum g_{CD} values decided by the equation, g_{CD} = 1/100 x γ_{PSS} x $g_{CD(100\%e.e.)}$ = 1/2($g_{CD(100\%e.e.)}$)^2.[19,31]

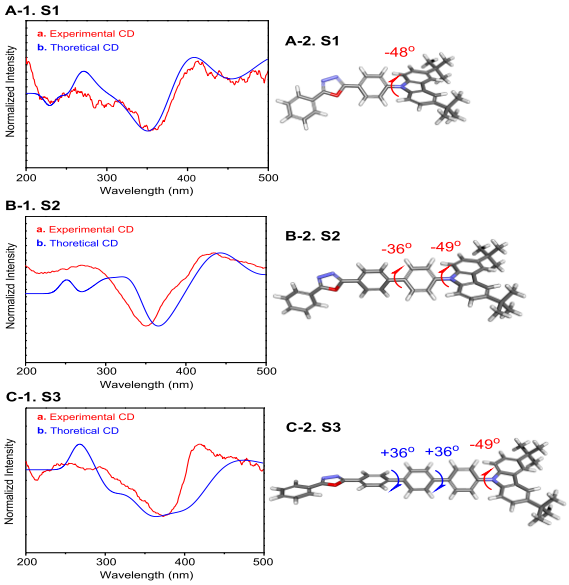

Fig. 3. Experimental CD spectra induced upon L-CPL irradiation (a) and theoretical CD spectra (b) for S1 [A-1], S2 [B-1], and S3 [C-1] and optimized conformations of the "wing" models with dihedral angles of S1 [A-2], S2 [B-2], and S3 [C-2].

In order to understand chiral structures of S1, S2, and S3 induced by CPL irradiation, their conformations and CD spectra were studied by theoretical calculations (Fig. 3). Through conformational optimization by DFT calculations at the B97D3/6-31G* level of theory,[35,36] the 1,3,5-tris(5-phenyl-1,3,4-oxadiazol-2-yl)benzene moiety ("core" group) was almost flat for all three molecules (Fig. S6 in ESI). Axial chirality of the outer parts of the molecules ("wings") should hence result in the observed CD spectra. Optimization of wing models indicated their probable conformations (Fig. 3 A-1, B-1, and C-1). As for S1, axial chirality is possible only for the *N*-phenylcarbazole moiety on the periphery. As for S2, the *N*-phenylcarbazole moiety and the central biphenyl moiety have the same handedness of axial chirality. As for S3, the *N*-phenylcarbazole moiety and the central terphenyl moiety have opposite handedness. The dihedral angle between the *N*-carbazolyl and the directly attached phenyl moieties was almost -48~49° for all three molecules.

The contribution of the wing groups to chirality was further evaluated through the prediction of the CD spectra by TD-DFT (Fig. 3 A-1, B-1, and C-1, blue curves). The theoretical spectra well coincided the experimental ones induced by R-CPL irradiation, suggesting that the optimized conformations may well represent the chiral conformations induced by R-CPL. Also, the experimental spectra of S1, S2, and S3 are overall similar to each other, showing a negative trough as the main band in the range of ca. 300-400 nm associated with a bisignet signal

centered at around 400 nm, which may indicate that the experimental spectra are based mainly on the axial chirality of the *N*-phenylcarbazole moiety common for the three molecules on the periphery of the molecules. Single-handed propeller-like chirality of the periphery of the molecules may thus be induced to the three molecules by CPL where R-CPL irradiation induced left-handed twist.

The bisignet signal centered at around 400 nm was well reproduced in the theoretical CD spectra of S1 and S2 while it was not for S3. This range of spectrum may be contributed also by chirality of the terphenyl moiety in S3, which was supported by the fact that theoretical CD spectral shape at around 400 nm changed according to alternations in dihedral angels in the terphenyl moiety (Fig. S7 in ESI). Conformations other than the one indicated in Fig.3. C-2 may also contribute to the real S3 film.

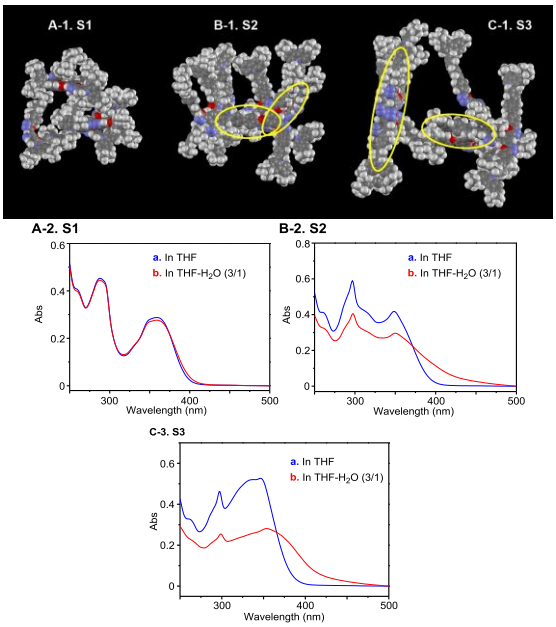

Fig. 4. Top: Aggregate structures of five molecules of S1 [A-1], S2 [B1], and S3 [C-1] observed through MD simulations in the presence of 1000 $CHCl_3$ molecules under an NPT ensemble at 300 K using periodic boundary conditions for 1 nsec. $CHCl_3$ molecules are omitted for clarity, and yellow ovals indicate π-stacked parts. Full model structures and enlarged views of π-stacking are found in Figs. S9 and S10, respectively, in ESI. Bottom: Absorbance spectra of S1 [A-2], S2 [B-2], and S3 [C-2] in THF (a) and in THF-H_2O (3/1, v/v) at 3.8 x 10^{-6} M in 1-cm cell.

Further, chirality induction was more efficient when a higher concentration of solution was used for film casting (Fig. S5 in ESI). In addition, the films showed weak optical textures under polarized microscopic observation which were clearer for the films prepared from higher-concentration solutions and for S2 and S3 than S1 (Fig. S11 in ESI). While the textures were not clear enough to be connected to any liquid crystals, the results are suggestive of some intermolecular aggregates formation. Moreover, chirality induction was not possible for an S2 film whose optical texture had been erased by heating at 320°C (Fig. S12 in ESI), suggesting that the proposed aggregates are indispensable in chirality induction though the molecules do not show any clear thermal transition except for glass transition.

In order to obtain information on this aspect, molecular dynamics (MD) simulations were conducted using periodic boundary conditions where five full models of the molecules were mixed with 1000 $CHCl_3$ molecules per cell to reproduce a solution for film fabrication (Fig. 4 A-1, B-1, and C-1, and Figs. S9 and S10 in ESI). Through the simulations, S2 and S3 formed loose aggregates with indefinite structures in which π-stacking was found. In contrast, S1 also formed an aggregate but showed no clear π-stacking. This point was supported by experimental absorbance spectra of the molecules in a mixture of tetrahydrofuran (THF) and H_2O (3/1, v/v) where H_2O should enhance aggregate formation (Fig. 4 A-2, B-2, and C-2). Whereas S2 and S3 showed remarkable hypochromism due to π-stacking, S1 did not. The fact that the maximum g_{CD} value observed on L-CPL irradiation was much greater for S2 and S3 than for S1 may arise from the difference in the extent of aggregate formation. Similar results were obtained also in $CHCl_3$-methanol mixture (Fig. S14 in ESI).

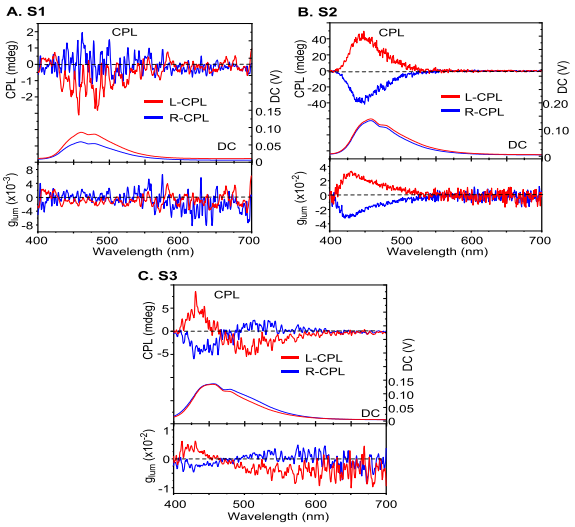

Fig. 5. Circularly polarized luminescence (top), DC (middle), and g_{lum} (bottom) spectra of S1 [A], S2 [B], and S3 [C] whose chirality was induced by CPL irradiation.

The CD-active films efficiently exhibited blue circularly polarized luminescence on photo excitation (Fig. 5). The efficiency of circularly polarized luminescence is evaluated in terms of the Kuhn's anisotropy factor for luminescence ($g_{lum} = 2(I_L - I_R)/(I_L + I_R)$ where I_L and I_R are intensities of left-handed and right-handed circularly polarized luminescence, respectively). The S1 films showed rather weak circularly polarized luminescence where exact values g_{lum} were not clear but the signs of circularly polarized luminescence were recognized to be opposite to those of the CD spectra. The S2 films showed very clear and intense, monotonous circularly polarized luminescence spectra with the maximum g_{lum} of ca. 3 x 10^{-2} at 440 nm where the signs of luminescence coincided with those of CD spectra. The S3 films also showed clear circularly polarized luminescence spectra having bisignet shapes with the maximum g_{lum} of ca. 3 x 10^{-3} at 425 nm where the signs of the lower-energy circularly polarized luminescence bands were opposite to those of CD spectra. Thus, the maximum g_{lum} values were about an order of magnitude higher than g_{CD} values for S2 and S3, and the sign of circularly polarized luminescence was inverted for S1 and S3, suggesting that chirality amplification took place for S2 and S3 and chirality inversion occurred for S1 and S3 in excited states. The bisignet luminescence spectral shapes of S3 may mean that chirality inversion of a part of the molecular structure or change in aggregation occurred in excited states. It could also arise from exciton coupling in aggregates.[37]

The induced chirality of S1-S3 films was stable at least for months at room temperature, for more than 72 h at 150 °C, for 60 min at 220 °C while it was quickly lost at 320 °C and on irradiation by intense non-polarized light (Fig. S8 in ESI). The molecules thus showed much high stability of chiral structures compared with general small molecules.

In conclusion, chirality was induced to S1, S2, and S3 in film by CPL irradiation where chirality amplification took place and the induction efficiency was much higher for S2 and S3 than S1. The molecules are considered to take preferred-handed propeller conformation of the *N*-phenylcarbazole moiety where R-CPL induces left-handed twist sense. The optically active films efficiently exhibited blue circularly polarized luminescence where chirality amplification and inversion took place in excited states.[38-41] S2 appeared superior to S3 in both chirality induction and circularly polarized emission while S3 seemed to exert more remarkable π-stacking. This could be explained in terms of the fact that S2 has one less Ar-Ar bond of axial chirality which can contribute to higher chiral structural uniformity within molecule as more Ar-Ar bonds could lead to a higher chance of chirality inversion. The balance between the number of Ar-Ar bonds and the extent of π-stacking might make S2 the most efficient molecule among the three. The chirality inversion of S1 and S3 in excited states could be ascribed to weaker π-stacking and lower chiral structural uniformity, respectively.

This work thus presented efficient chirality induction to the amorphous molecules by CPL through chirality amplification. This is in a sharp contrast to the fact that efficient chirality amplification has been shown mainly for the systems having highly ordered intermolecular or surface structures.[15-19,24-28] Furthermore, the CPL irradiation method led to much more facile preparation of blue circularly polarized luminescent materials compared with the synthesis in the existing examples.[42-45]

This work was supported in part by the MEXT/JSPS KAKENHI Grant Number JP 19H02759 and in part by the JST grant No. JPMJTM19E4. Technical Division of ICAT, Hokkaido University is.

Conflicts of interest

There are no conflicts to declare.

Notes and references

1 I. Ojima, *Catalytic Asymmetric Synthesis*, John Wiley & Sons, 2nd ed. **2010**.
2 E. Yashima, N. Ousaka, D. Taura, K. Shimomura, T. Ikai, and K. Maeda, *Chem. Rev.,* **2016**, *116*, 13752−13990.
3 T. Nakano, Y. Okamoto, *Chem. Rev.* **2001**, *101*, 4013–4038.
4 J. A. Le Bell, *Bull. Soc. Chim. Fr.* **1874**, *22*, 337–347.
5 J. H. Van't Hoff, *Pamphlet* **1874**, September 3.
6 H. Rau, *Chem. Rev.* **1983**, *83*, 535-547.
7 Y. Inoue, *Chem. Rev.* **1992**, *92*, 741–770.
8 B. L. Feringa, R. A. Delden, *Angew. Chem. Int. Ed.* **1999**, *38*, 3418–3438.
9 T. Kawasaki, M. Sato, S. Ishiguro, T. Saito, Y. Morishita, I. Sato, H. Nishino, Y. Inoue, K. Soai, *J. Am. Chem. Soc.* **2005**, *127*, 3274–3275.
10 K. Soai, T. Shibata, H. Morioka, K. Choji, *Nature* **1995**, *378*, 767–768.
11 C. He, G. Yang, Y. Kuai, S. Shan, L. Yang, J. Hu, D. Zhang, Q. Zhang, G. Zou, *Nat. Commun.* **2018**, *9*, 1-8.
12 C. He, Z. Feng, S. Shan, M. Wang, X. Chen, G. Zou, *Nat. Commun.*, **2020**, *11*, 1188.
13 J. Yeom, B. Yeom, H. Chan, K. W. Smith, S. Dominguez-Medina, Joong H. Bahng, G. Zhao, W.-S. Chang, S.-J. Chang, A. Chuvilin, D. Melnikau, A. L. Rogach, P. Zhang, S. Link, P. Král and N. A. Kotov, *Nat. Mater.*, **2015**, *14*, 66-72.
14 X. He, L. Chen, Y. Zhao, H. Chen, S. C. Ng, X. Wang, X. Sun, *Org. Electron.* **2016**, *37*, 14-23.
15 Y. Wang, T. Sakamoto, T. Nakano, *Chem. Commun.*, **2012**, *48*, 1871-1873.
16 Y. Wang, T. Harada, L. Q. Phuong, Y. Kanemitsu, T. Nakano, *Macromolecules* **2018**, *51*, 6865-6877.
17 A. Pietropaolo, Y. Wang, T. Nakano, *Angew. Chem. Int. Ed.* **2015**, *127*, 2726-2730.
18 Y. Wang, A. L. Kanibolotsky, P. J. Skabara, T. Nakano, *Chem. Commun.* **2016**, *52*, 1919-1922.
19 T. Nakano, *Chem. Rec.* **2014**, *14*, 369-385.
20 A. Imamura, R. Hoffmann, *J. Am. Chem. Soc.* **1968**, 90, 5379–5385.
21 T. Sakamoto, Y. Fukuda, S. Sato and T. Nakano, *Angew. Chem. Int. Ed.* **2009**, *48*, 9308-9311.
22 A. Pietropaolo, T. Nakano, *J. Am. Chem. Soc.* **2013**, *135*, 5509-5512.
23 A. Pietropaolo, T. Nakano, *Chirality* **2020**, 1-6.
24 L. Nikolova, T. Todorov, M. Ivanov, F. Andruzzi, S. Hvilsted, P. S. Ramanujam, *Opt. Mater. (Amsterdam)* **1997**, *8*, 255–258
25 G. Iftime, F. L. Labarthet, A. Natansohn, P. Rochon, *J. Am. Chem. Soc.* **2000**, *122*, 12646–12650.
26 A. Natansohn, P. Rochon, *Adv. Mater.* **1999**, 11, 1387–1391.
27 M. Fujiki, K. Yoshida, N. Suzuki, J. Zhang, W. Zhang, X. Zhu, *RSC Adv.* **2013**, *3*, 5213-5219.
28 L. Wang, L. Yin, W. Zhang, X. Zhu, M. Fujiki, *J. Am. Chem. Soc.* **2017**, 139, 13218-13226.
29 M.-J. Kim, S.-J. Yoo, D.-Y. Kim, *Adv. Funct. Mater.*, **2006**, *16*, 2089-2094.
30 J. Kim, J. Lee, W. Y. Kim, H. Kim, S. Lee, H. C. Lee, Y. S. Lee, M. Seo S. Y. Kim, *Nat. Commun.*, 2015, **6**, 1-8.
31 J. Li, G. B. Schuster, K.-S. Cheon, M. M. Green, J. V. Selinger, *J. Am. Chem. Soc.* **2000**, *122*, 2603–2612.
32 A. Pietropaolo, C. Cozza, Z. Zhang, T. Nakano, *Liq. Cryst.* **2018**, *45:13-15*, 2048-20531-6.
33 T. Nakano, T. Yade, *J. Am. Chem. Soc.* **2003**, 125, 15474-15484.
34 W. Kuhn, *Trans. Faraday Soc.* **1930**, *26*, 293–308.
35 S. Grimme, *J. Comp. Chem*. **2006**, *27*, 1787-1799.
36 S. Grimme, S. Ehrlich, L. Goerigk, *J. Comp. Chem*. **2011**, *32*, 1456-1465.
37 S. T. Duong, M. Fujiki, *Polym. Chem.*, **2017**, *8*, 4673-4679.
38 H. Tanaka, Y. Inoue, T. Mori, *ChemPhotoChem*, **2018**, *2*, 386-402.
39 J. Kumar, T. Nakashima, T. Kawai, **2015**, *6*, 3445-3452.
40 Y. Sang, J. Han, T. Zhao, P. Duan, M. Liu, *Adv. Mater.*, **2020**, *32*, 1900110.
41. W. Chen, K. Ma, P. Duan, G. Ouyang, X. Zhu, L. Zhang, M. Liu, *Nanoscale*, 2020, **12**, 19497-19515.
42 D.-Q. He, H.-Y. Lu, M. Li, C.-F. Chen, *Chem. Commun.* **2017**, *53*, 6093-6096.
43 C. Schaack, L. Arrico, E. Sidler, M. Górecki, L. Di Bari, F. Diederich, *Chem. Eur. J.* **2019**, *25*, 8003-8007.
44 N. Sharma, E. Spuling, C. M. Mattern, W. Li, O. Fuhr, Y. Tsuchiya, C. Adachi, S. Bräse, I. D. Samuel and E. Zysman-Colman, *Chem. Sci*. **2019**, *10*, 6689-6696.
45 T. Ono, K. Ishihama, A. Taema, T. Harada, K. Furusho, M. Hasegawa, Y. Nojima, M. Abe, Y. Hisaeda, *Angew. Chem. Int. Ed.* **2020**. https://doi.org/10.1002/anie.202011450.

